Journal of Physics: Conference Series

PAPER • **OPEN ACCESS**

Hydrogen molecular ions: new schemes for metrology and fundamental physics tests

To cite this article: Jean-Philippe Karr *et al* 2016 *J. Phys.: Conf. Ser.* **723** 012048

View the article online for updates and enhancements.

Related content

- Defining and Measuring Nature: Measurement in the Early Modern Period
J H Williams
- Metrology in Pharmaceutical Industry - A Case Study
Priscila D. Yuvamoto, Ricardo K. S. Fermam and Elizabeth S. Nascimento
- Coherence modulation at the photon-counting level: A new scheme for secure communication
William T Rhodes, Abdellatif Boughanmi and Yezid Torres Moreno

Recent citations

- Leading-order relativistic corrections to the rovibrational spectrum of H2+ and HD+ molecular ions
D. T. Aznabayev *et al*
- Prospects for a polar-molecular-ion optical probe of varying proton-electron mass ratio
Mark G. Kokish *et al*
- Universal interrogation protocol with zero probe-field-induced frequency shift for quantum clocks and high-accuracy spectroscopy
T. Zanon-Willette *et al*



IOP ebooks™

Bringing you innovative digital publishing with leading voices to create your essential collection of books in STEM research.

Start exploring the collection - download the first chapter of every title for free.

This content was downloaded from IP address 131.169.95.213 on 14/02/2019 at 14:07

Hydrogen molecular ions: new schemes for metrology and fundamental physics tests

Jean-Philippe Karr[1,2], Sayan Patra[3], Jeroen C J Koelemeij[3], Johannes Heinrich[1], Nicolas Sillitoe[1], Albane Douillet[1,2], and Laurent Hilico[1,2]

[1] Laboratoire Kastler Brossel, UPMC-Sorbonne Universités, CNRS, ENS-PSL Research University, Collège de France, 4 place Jussieu, F-75005 Paris, France
[2] Université d'Evry-Val d'Essonne, Boulevard François Mitterrand, F-91000 Evry, France
[3] LaserLaB and Department of Physics & Astronomy, VU University, De Boelelaan 1081, 1081 HV Amsterdam, The Netherlands

E-mail: karr@lkb.upmc.fr

Abstract. High-accuracy spectroscopy of hydrogen molecular ions has important applications for the metrology of fundamental constants and tests of fundamental theories. Up to now, the experimental resolution has not surpassed the part-per-billion range. We discuss two methods by which it could be improved by a huge factor. Firstly, the feasibility of Doppler-free quasi-degenerate two-photon spectroscopy of trapped and sympathetically cooled ensembles of HD^+ ions is discussed, and it is shown that rovibrational transitions may be detected with a good signal-to-noise ratio. Secondly, the performance of a molecular quantum-logic ion clock based on a single Be^+-H_2^+ ion pair is analyzed in detail. Such a clock could allow testing the constancy of the proton-to-electron mass ratio at the 10^{-17}/yr level.

1. Introduction

It has long been suggested that high-resolution spectroscopy of rovibrational transitions in the hydrogen molecular ions H_2^+ and HD^+ can provide an accurate value of the proton-electron mass ratio μ [1, 2]. Recently, a measurement of the $(v, L) : (0, 2) \rightarrow (8, 3)$ vibrational overtone in trapped, cold HD^+ allowed the first determination of μ from molecular vibrations [3] with a relative uncertainty of 2.9×10^{-9} that is mainly limited by Doppler broadening. A promising avenue for further improvement is Doppler-free two-photon spectroscopy [4]; an experiment to probe the $(0, 2) \rightarrow (1, 2)$ transition in H_2^+ is being set up at LKB Paris [5]. We describe an alternative scheme for two-photon spectroscopy of HD^+ with quasi-degenerate counterpropagating photons [6]. The lasers are tuned close to resonance with an intermediate rovibrational level in order to enhance the transition probability, thus avoiding the use of a build-up cavity; the residual first-order Doppler broadening is moreover suppressed by the two-photon Lamb-Dicke effect. The application of this technique to the $(0, 3) \rightarrow (4, 2) \rightarrow (9, 3)$ transitions at 1.44 μm, currently underway at VU University Amsterdam, is discussed in Section 2.
Hydrogen molecular ions were also proposed for the realization of optical molecular clocks with the aim of testing of the time variation of μ [7]. The most stringent laboratory constraints on the $\dot{\mu}/\mu$ variation rate come from frequency comparisons between optical and Cs clocks [8, 9]. The current uncertainty level, slightly above 10^{-16}/yr, is mainly limited by the performance of


Content from this work may be used under the terms of the Creative Commons Attribution 3.0 licence. Any further distribution of this work must maintain attribution to the author(s) and the title of the work, journal citation and DOI.
Published under licence by IOP Publishing Ltd

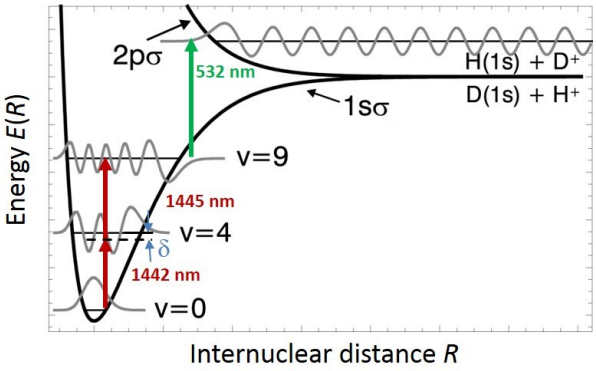


Figure 1. (colour online) Schematic of quasi-degenerate two-photon spectroscopy of the $(v, L) : (0, 3) \rightarrow (9, 3)$ transition in HD^+ (the hyperfine structure of the rovibrational levels is not shown). The transition is detected by resonance-enhanced multiphoton dissociation (REMPD) using an additional laser at 532 nm; the REMPD signal is the fractional loss of HD^+ ions.

Cs standards. A direct frequency ratio measurement between atom- and molecule-based optical clocks would overcome this limitation and enable a nearly pure measurement of $\dot{\mu}/\mu$, independent of variations of the fine structure constant $(\dot{\alpha}/\alpha)$. This motivates the construction of a molecular clock with accuracy and stability reaching the 10^{-17} range. A large number of molecular lines with greatly enhanced sensitivity to μ variations have been discovered over the last decade (see [10] for a review). However, the proposed transitions are often rather exotic in the sense that they involve highly excited states in complex molecules, so that efficient preparation of the initial state is very challenging. The potential of rovibrational transitions from low-lying levels of simple molecules such as H_2^+ and HD^+ [7, 11, 12] or N_2^+ [13, 14], where efficient state preparation by multiphoton ionization has been demonstrated, is thus worth investigating. In Section 3 we discuss the performance of quadrupole transitions in H_2^+. While possible clock transitions in this system were studied in Refs. [11, 12], we bring the discussion further in two main respects. First, important practical considerations for the clock's operation, namely its stability and the requirement of highly efficient internal state preparation of the molecular ions, lead us to select different transitions. Second, we analyze an alternative scheme to cancel the electric quadrupole and quadratic Zeeman shifts, which gave the main contribution to the error budget in [11], and show that it allows improving the clock's accuracy.

2. Two-photon spectroscopy of trapped HD^+ ion ensembles

The spectroscopic scheme for quasi-degenerate two-photon spectroscopy of trapped and sympathetically cooled HD^+ ions is shown in figure 1. Its feasibility was carefully studied in Ref. [6] by solving the optical Bloch equations in the framework of a four-level model. The first three levels are hyperfine sublevels of the $(v, L) = (0, 3)$, $(4, 2)$ and $(9, 3)$ levels respectively, and the fourth one is a virtual level whose population represents the photodissociated fraction, i.e. the REMPD signal. An underlying assumption is that the chosen hyperfine sublevel of the intermediate state $(4, 2)$ is well-isolated, more precisely, that the detuning δ with respect to the one-photon resonance (see figure 1) can be made smaller than the separation with neighboring hyperfine levels. The Zeeman structure is not included, because the linewidths of both 1.4 μm lasers are supposed to be larger than the Zeeman splitting so as to address all Zeeman sublevels and enhance the signal. The Doppler-broadened one-photon lineshape is accurately modeled by injecting realistic ion trajectories from molecular dynamics simulations in the Bloch equations. The following results were established:

(i) Maximal visibility of the Doppler-free signal is achieved for a detuning δ slightly above the Doppler width of the single-photon transitions. Indeed a smaller detuning increases the two-photon transition rate, but δ should remain sufficiently large to avoid competition

from the sequential excitation process.

(ii) The two-photon peak is power broadened, with a width of a few hundred Hz at the onset of saturation of the REMPD signal. There is also a lightshift of the order of a few Hz, which can however be canceled if the Rabi frequencies of both single-photon transitions are made equal.

(iii) In order to predict the observed signal in actual experiments where the HD^+ ions are distributed over rotational and hyperfine states within the ground vibrational state $v = 0$, the REMPD rate extracted from the four-level model is included into a set of rate equations describing population redistribution among rotational and hyperfine states by blackbody radiation. The latter enhances the REMPD signal since it continuously recycles ions into the lower state of the transition. It is found that the photodissociated fraction can be made significantly larger than the measurement noise observed in [3].

Quasi-degenerate two-photon spectroscopy of HD^+ thus appears feasible and could reach an accuracy level of about 10^{-14} [6]; the experiment is underway at VU University Amsterdam. We now discuss the choice of suitable hyperfine components. As pointed out in (i) above, it is important to choose the detuning δ away from any transition to intermediate hyperfine levels in $v = 4, L = 2$ by at least the Doppler width. In this way, the first photon of the two-photon transition does not significantly populate any of the intermediate levels, which suppresses the unwanted background signal due to stepwise excitation from $v = 0$ to $v = 9$ via $v = 4$. A good indicator of this suppression factor is the one-photon spectrum of the $(v, L) : (0, 3) \rightarrow (4, 2)$ transition at 1442 nm, shown in figure 2. Assuming that the second photon always leads to immediate REMPD - which is a worst case scenario - this spectrum essentially represents the maximum expected background signal due to population in $v = 4$ as a function of the frequency of the first photon. Spectra are shown for two different values of the temperature corresponding to the range of temperatures obtained in previous experiments with the same ion trap [3]. Note that in Ref. [6], ion trajectories are obtained from simulations of sympathetic cooling in an ideal trap, leading to lower temperatures.

Apart from choosing δ such that the maximum expected background signal (figure 2) is low, the strength of the hyperfine component should be as large as possible, and the Zeeman shift as low as possible in order to address all Zeeman components with a narrow-line laser. Figure 2 indicates that several such lines may be probed with sufficient signal-to-noise ratio with intermediate-level detunings of 15-30 MHz. Note that the full two-photon $(v, L) : (0, 3) - (4, 2) - (9, 3)$ Doppler-broadened spectrum may actually be less broadened than the $(v, L) : (0, 3) \rightarrow (4, 2)$ transition due to hyperfine state selection during the first step of the excitation. Consequently, even smaller intermediate-level detunings might be feasible. Future work will address the precise shape of the full two-photon spectrum (i.e. both the direct and stepwise contributions) using an extended version of the rate equation approach of Ref [3].

3. Performance of an H_2^+ clock

Before addressing the leading systematic effects affecting an optical clock based on hydrogen molecular ions and the accuracy level at which they can be controlled, other characteristics that influence the choice of suitable rovibrational transitions need to be considered. The first one is the clock's stability, which determines the required integration time to measure the $\dot{\mu}/\mu$ variation rate at the 10^{-17}/yr level. The main source of noise in single-ion clocks is the quantum projection noise, setting a stability limit that is inversely proportional to the clock frequency and to the square root of the interrogation time (see e.g. [15]). This implies, firstly, that the stability limit is lower in HD^+ than in H_2^+ due to the lower lifetimes of the rovibrational states ($\tau \sim 15 - 55$ ms for $v = 1 - 4$ [16], whereas $\tau \sim 10^6$ s in H_2^+ [17]) which limit the interrogation time; this is why we only consider H_2^+ in the following. Secondly, all other characteristics being equal, one should

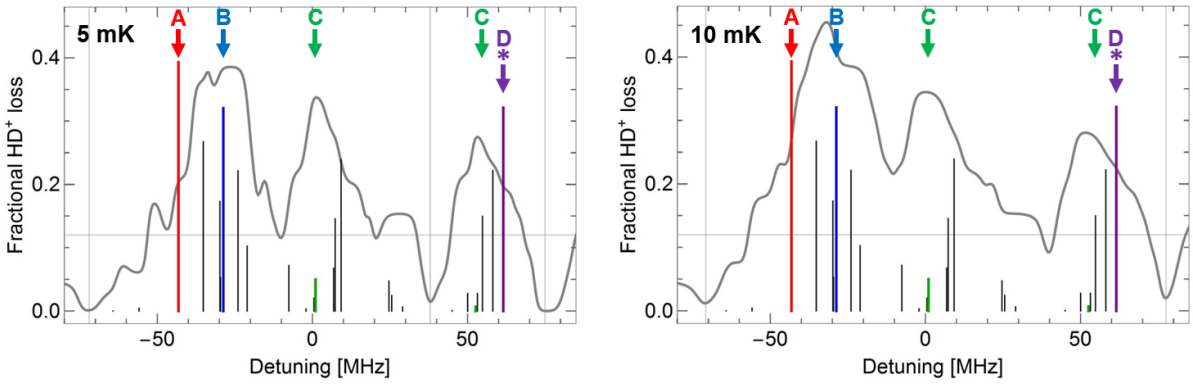


Figure 2. (colour online) Calculated Doppler-broadened single-photon spectra of the (v, L) : $(0, 3) \rightarrow (4, 2)$ transition at 1442 nm, assuming detection by REMPD. Doppler-broadening, saturation (due to the finite HD^+ sample size) and population redistribution by blackbody radiation lead to a rich spectrum (gray curve). The spectra were calculated for an interrogation time of 10 s, an ambient blackbody radiation temperature of 300 K, and an HD^+ ion temperature of 5 mK (left panel) and 10 mK (right panel) using the method described in Refs. [3, 6]. The underlying hyperfine transitions are indicated by the vertical black sticks. Possible intermediate steps for enhanced two-photon transitions are indicated by the thick vertical sticks and arrows. Transitions with (from left to right) $F = 1$, $S = 2$, and $J = 5$ to $J' = 4$ (A), $F = 1$, $S = 1$, and $J = 4$ to $J' = 3$ (B), and $F = 1$, $S = 2$, and $J = 1$ to $J' = 0, 2$ (C) were identified in [6] as having very small Zeeman shifts at the 10-Hz level (for a 0(2) μT magnetic field, realized with three pairs of external magnetic field coils while using the fluorescence of the Be^+ ions as a magnetic field probe). The line which may be probed with the lowest detuning, i.e. $F = 0$, $S = 1$, and $J = 4$ to $J' = 3$ (D) is labeled with a star. It exhibits a larger Zeeman broadening of 1.5 kHz, but the net Zeeman shift is below 1 Hz. The gray horizontal line indicates the expected achievable two-photon signal (which depends on line strengths and is adjustable through the laser intensity), and vertical gray lines indicate suitable laser detunings for which the Doppler-broadened background will be considerably smaller than the two-photon signal.

look for transitions with the highest possible frequency, i.e. vibrational overtones. Another important feature is the possibility of efficient state preparation in the lower rovibrational and hyperfine state by resonant-enhanced multiphoton ionization (REMPI). H_2^+ ion production in selected rovibrational states with $\sim 90\%$ selectivity has been reported [18], but the population of hyperfine sublevels has not been addressed, which is why it seems preferable to choose levels with the simplest possible hyperfine structure, i.e. $L = 0$ (no structure) or $L = 2, 4...$ (2 sublevels). Finally, one-photon quadrupole transitions have been shown to be more promising than two-photon transitions as the latter have lower frequencies and are affected by larger lightshifts [12].

Some of the main systematic shifts lend themselves to efficient cancellation strategies. It was pointed out that the mean frequency of transition pairs between "stretched states", $(v, L, J = L + 1/2, M_J = \pm(L + 1/2)) \rightarrow (v', L', J' = L' + 1/2, M'_J = \pm(L' + 1/2))$ is free of both linear and quadratic Zeeman shifts [12, 19]; here L is assumed to be an even number, so that the total nuclear spin is zero, and $\mathbf{J} = \mathbf{L} + \mathbf{s_e}$ is the total angular momentum. The quadrupole shift [20] can be nulled by measuring the transition frequencies for three orthogonal directions of the magnetic field [21]. The level of cancellation with this method is limited by the inaccuracy in setting the magnetic field directions, and the quadrupole shift remains the most important limitation of the clock's accuracy unless a cancellation occurs between the lower and

upper levels. The latter consideration led to single out the $(v, L) : (0, 4) \rightarrow (2, 2)$ transition at $\lambda = 2.61$ μm [12], whose uncertainty budget is studied in more detail hereafter. We also analyze a different method based on the measurement of several symmetric pairs of Zeeman subcomponents, inspired from previous work in atomic clocks [22] where it was shown to yield a much higher degree of cancellation, in addition to nulling the linear Zeeman shift and the tensor part of the Stark shift. This approach is also applicable in H_2^+ since the quadrupole shift has the same form proportional to $J(J+1) - 3M_J^2$ [20]. However, in contradistinction with the "stretched states" case, the quadratic Zeeman shift is not suppressed and could limit the achievable performance. To solve this issue, we propose averaging instead over *all* the Zeeman subcomponents of the hyperfine structure of the involved rovibrational levels. The quadratic Zeeman shift, which essentially originates from couplings within the hyperfine structure, will then be nulled to a very high degree, while the cancellation of the linear Zeeman shift is preserved. In view of the small hyperfine splitting of even-L states ($\Delta\nu_{\rm hfs} \sim 100$ MHz [24]) all the transitions can be interrogated with a single laser. To sum it up, we select the following transitions:

- the pair $(v = 0, L = 4, J = 9/2, M_J = \pm 9/2) \rightarrow (v = 2, L = 2, J = 5/2, M_J = \pm 5/2)$, for its extremely low quadrupole shift and suppressed Zeeman shift;
- the transitions $(v = 0, L = 0, J = 1/2, M_J = \pm 1/2) \rightarrow (v', L' = 2, J', \pm M_J')$ for canceled quadrupole and Zeeman shifts. We choose $L = 0$ and $L' = 2$ firstly in order to have the simplest possible Zeeman structure, and secondly because the absence of hyperfine structure for $L = 0$ favors efficient state preparation. Five transition pairs are needed for averaging over all states, but this is actually not necessary as a shift-independent frequency can be deduced from the measurement of only three transition pairs (see table 2), exploiting the known dependence of the quadrupole shift on J and M_J.

Our results are summarized in tables 1 and 2. We briefly describe below the methods and hypotheses we have used to estimate the magnitude and residual uncertainties of the leading frequency shifts.

(i) Quadrupole shift. The quadrupole moment of the $(v = 0, L = 0)$ state is zero, and those of the $(v', L = 2)$ states are taken from [20]. As already discussed in [12], those of the $(0, 4)$ and $(2, 2)$ states, which are very close to each other, were recalculated independently in a three-body approach to get a more precise estimate of the quadrupole shift. The latter is evaluated for an electric field gradient $V_{zz} = 0.67 \times 10^8$ V/m^2, similarly to [11, 12]. For the $(0, 4) \rightarrow (2, 2)$ transition, the residual uncertainty is equal to 1 percent of the shift, as is typically obtained with the B-averaging method. For the three $L = 0 \rightarrow L' = 2$ transitions, assuming that the M_J-averaging method is used we take an uncertainty equal to 10^{-4} times the shift of the most sensitive states, that are the $|M_J| = 5/2$ states. This is a conservative estimate, as an even better level of cancellation was demonstrated in [23].

(ii) Quadratic Zeeman shift. Results of calculations of this shift are reported in [11]. However, we performed independent calculations since the transitions considered here were not included in that reference. Quadratic Zeeman coefficients are obtained by diagonalizing $H = H_{hfs} + H_Z$ where H_{hfs} is the hyperfine structure Hamiltonian [24] and H_Z is the Zeeman Hamiltonian [25] (see also [19]). A first contribution comes from the magnetic field associated with blackbody radiation (BBR); BBR frequencies being much higher than the hyperfine splitting, the resulting shift is very small [26] and may be neglected. The second contribution is from the background magnetic field, for which we choose a small value of 2 μT to reduce the magnitude of the shift. Such a residual field can typically be obtained by building the trap structure with nonmagnetic materials [23]. Similarly to the quadrupole shift, the averaging method we propose for the quadratic Zeeman shift is conservatively assumed to result in cancellation by four orders of magnitude. Note that the averaged shift

is not strictly zero due to couplings to other vibrational levels, but such contributions are estimated to be smaller than 10^{-19}.

(iii) Blackbody radiation (Stark) shift. This shift was calculated in [27] for the rovibrational levels of H_2^+. An experimental uncertainty of 5 K on the 300 K BBR temperature is assumed.

(iv) AC Stark shift. The calculation of the lightshift induced by the clock laser is described in [12]; here its expression is slightly different since the tensor part is nulled by the M-averaging procedure:

$$\Delta f_{LS} = -\frac{m_e \lambda^2}{4h} \frac{\Delta\alpha^{if(0)}}{\tau^2 |\Theta^{if}_{\varepsilon,n}|^2}. \quad (1)$$

where m_e is the electron's mass, λ the transition wavelength, $\Delta\alpha^{if(0)} = \alpha^{(0)}_{v',L'} - \alpha^{(0)}_{v,L}$ the dimensionless dynamic *scalar* polarizability difference, τ the duration of the clock's interrogation π-pulse, and $\Theta^{if}_{\varepsilon,n}$ the dimensionless quadrupole transition amplitude, which depends on the propagation direction $\mathbf{n}$ and polarization $\boldsymbol{\varepsilon}$. The latter are adjusted to maximize the amplitude of the weakest Zeeman components. We assume an interrogation time $\tau = 100$ ms [28, 29] and a residual uncertainty equal to 1% of the shift.

(v) Second-order Doppler shift. This is one of the crucial limitations, due to the light mass of H_2^+. For example, in the Al^+/Mg^+ clock the residual uncertainty for this effect is 7.8×10^{-18}; a similar level of control on the trapped ion's residual kinetic energy would lead to a 1×10^{-16} uncertainty in the case of H_2^+. In view of ongoing efforts to improve micromotion minimization techniques further [31], an uncertainty level of 1×10^{-17} may realistically be achieved.

Two other systematic effects were omitted in tables 1 and 2 as they do not contribute significantly to the error budget:

(vi) Scalar Stark shift induced by trap fields. The Stark and second-order Doppler shifts associated with micromotion, being driven by the same electric field, are correlated and should be considered together. According to Eqs. (14) and (24) of [23], the ratio of the Stark and Doppler shifts is given by

$$\frac{\Delta\nu_s}{\Delta\nu_D} = \frac{\Delta\alpha_0}{\hbar\omega_0} \left(\frac{m\Omega c}{e}\right)^2 \quad (2)$$

where $\hbar\omega_0$ is the transition energy , m the H_2^+ ion's mass, Ω the trap frequency and $\Delta\alpha_0$ the static scalar polarizability difference. With the value $\Omega = 2\pi \times 59$ MHz [28, 29] and static polarizabilities from [27], this ratio lies between 0.0014 and 0.002 for the transitions under consideration. The scalar Stark shift thus may be safely neglected.

(vii) Tensor Stark shifts from the clock laser and from trap fields. They are of the same order as the related scalar shifts (as can be seen by comparing scalar and tensor polarizability differences e.g. in table 3 of [12]). Similarly to the quadrupole shift, they are canceled by about four orders of magnitude by the M_J-averaging method [23], and their residual uncertainties are thus negligible with respect to scalar contributions.

Examination of table 1 shows that an accuracy level of a few 10^{-17} represents a realistic goal for an H_2^+ ion clock, using either the $v = 0 \to 1$ transition at 4.24 μm, or the $v = 0 \to 2$ transitions at 2.27 and 2.61 μm. The $v = 0 \to 3$ transition at 1.58 μm would be an ideal choice from the point of view of laser and frequency measurement technology, but as the transitions become weaker with increasing Δv the AC stark shift strongly limits the achievable accuracy. While generalizations of the Ramsey interrogation scheme have been developed to improve light shift cancellation [30], their implementation in a quantum-logic ion clock is challenging. However,

Transition	$(0,4) \to (2,2)$		$(0,0) \to (1,2)$		$(0,0) \to (2,2)$		$(0,0) \to (3,2)$	
Frequency (THz)	114.99		70.64		132.25		190.18	
Source	shift	uncert.	shift	uncert.	shift	uncert.	shift	uncert.
Quadrupole shift	0	0.049	0	1.7	0	1.0	0	0.82
Quadr. Zeeman shift	< 0.01	< 0.01	< 0.01	1.1	< 0.01	0.61	< 0.01	0.46
Blackbody radiation	-12	0.80	-9.3	0.62	-11	0.74	-13	0.88
AC Stark shift	-220	2.2	-5.0	0.050	-200	2.0	-4500	45
Total uncertainty		2.6		2.4		2.7		45

Table 1. Estimated uncertainty budget for quadrupole rovibrational transitions in H_2^+, in parts in 10^{17}. The total uncertainty in the last line also includes a 1.0×10^{-17} contribution from the second-order Doppler shift (see text) and is obtained by adding all contributions quadratically.

M_J	J'	M'_J	$\Delta f_Z^{(1)}$	$\Delta f_Z^{(2)}$	Δf_Q
$\pm 1/2$	3/2	$\pm 1/2$	∓ 33.6 kHz	8.1 Hz	-9.7 Hz
$\pm 1/2$	5/2	$\pm 1/2$	∓ 22.4 kHz	-8.1 Hz	-11.1 Hz
$\pm 1/2$	5/2	$\pm 5/2$	∓ 27.8 Hz	0	13.8 Hz

Table 2. Detailed frequency shifts of the three individual transition pairs to be measured, in the case of the $(v, L) = (0, 0) \to (2, 2)$ transition. $\Delta f_Z^{(1)}$ and $\Delta f_Z^{(2)}$ are respectively the linear and quadratic Zeeman shifts for a 2 μT B-field. Δf_Q is the quadrupole shift for a field gradient $V_{zz} = 0.67 \times 10^8$ V/m^2. The BBR and scalar AC Stark shift (which are the same for all transitions) respectively amount to -14.7 and -163 mHz. The tensor part of the AC Stark shift (not given here) plays a negligible role since it is of the same order as the scalar part, but is nulled to a much higher degree by the averaging procedure. The shift-independent frequency is $\nu_0 = [3\nu(J' = 5/2, M'_J = \pm 5/2) + \nu(J' = 5/2, M'_J = \pm 1/2) + \nu(J' = 3/2, M'_J = \pm 1/2)]/5$ where $\nu(J', \pm M'_J)$ is itself the averaged frequency of two opposite Zeeman subcomponents. The hyperfine structure splitting between $J' = 3/2$ and $J' = 5/2$ is 92.7 MHz [24].

we note that according to Eq. (1) the lightshift scales like $1/\tau^2$. The $\Delta v = 3$ transition thus becomes practicable if longer interrogation times can be used; for example $\tau = 500$ ms would bring the overall uncertainty down to 2.4×10^{-17}. Finally, it is worth pointing out that, apart from the second-order Doppler shift, residual uncertainties associated with the various effects have been estimated conservatively and may be reduced further, down to the 1.0×10^{-17} mark or even below.

4. Conclusion

The schemes that have been discussed have the potential to improve the current accuracy of molecular ion spectroscopy by several orders of magnitude, with important outcomes in the field of fundamental metrology. Quasi-degenerate two-photon spectroscopy of HD^+ may ultimately reach an accuracy level of 10^{-14} or better; 10^{-12} would actually be sufficient for comprehensive tests of molecular QED theory [32] and an improved determination of the proton-to-electron mass ratio [33]. It is worth noting that this method may be applied to other molecular ions, where similar quasi-coincidences in the rovibrational spectrum are likely to occur. The second possibility, i.e. the realization of an H_2^+ optical clock, is much more challenging. Our accuracy estimates show that it may allow for tests of μ time variation at the 10^{-17}/yr level, improving current limits by one order of magnitude. The main drawback of H_2^+ is its light mass causing a larger second-order Doppler shift. On the plus side, this also leads to higher vibrational transition frequencies, allowing for better clock stability. Finally, a clock based on H_2^+ would represent, like

atomic hydrogen masers, a clock with a 'calculable' frequency, in this case providing a direct, 11-digit link from the SI second to the values of fundamental physical constants. Unlike H masers, however, an H_2^+ clock would operate at optical wavelengths and benefit from many of the techniques developed for ion-based optical atomic clocks.

Acknowledgements
The authors are grateful to V.I. Korobov and D. Bakalov for helpful discussions. This work was funded through the Dutch-French bilateral Van Gogh Programme. J.C.J.K. and S.P. thank the Netherlands Organization for Scientific Research (NWO), the Netherlands Technology Foundation (STW), and the Netherlands Foundation for Fundamental Research on Matter (FOM) for support. J.-Ph.K., J.H., N.S., A.D. and L.H. acknowledge funding from Agence Nationale de la Recherche (grant ANR-13-IS04-0002-01) and the European Commission under the Seventh Framework Programme FP7 GA 607491 COMIQ. J.-Ph.K. acknowledges support as a fellow of the Institut Universitaire de France.

References

[1] Wing W H, Ruff G A, Lamb Jr W E and Spezeski J J 1976 *Phys. Rev. Lett.* **36** 1488
[2] Bressel U, Borodin A, Shen J, Hansen M, Ernsting I and Schiller S 2012 *Phys. Rev. Lett.* **108** 183003
[3] Biesheuvel J, Karr J Ph, Hilico L, Eikema K S E, Ubachs W and Koelemeij J C J 2016 *Nature Comm.* **7** 10385
[4] Karr J Ph, Kilic S and Hilico L 2005 *J. Phys. B* **38** 853
[5] Karr J Ph, Bielsa F, Douillet A, Pedregosa Gutierrez J, Korobov VI and Hilico L 2008 *Phys. Rev. A* **77** 063410
[6] Tran V Q, Karr J Ph, Douillet A, Koelemeij J C J and Hilico L 2013 *Phys. Rev. A* **88** 033421
[7] Schiller S and Korobov V 2005 *Phys. Rev. A* **71** 032505
[8] Godun R M, Nisbet-Jones P B R, Jones J M, King S A, Johnson L A M, Margolis H S, Szymaniec K, Lea S N, Bongs K and Gill P 2014 *Phys. Rev. Lett.* **113** 210801
[9] Huntemann N, Lipphardt B, Tamm Chr, Gerginov V, Weyers S and Peik E 2014 *Phys. Rev. Lett.* **113** 210802
[10] Jansen P, Bethlem H L and Ubachs W 2014 *J. Chem. Phys* **140** 010901
[11] Schiller S, Bakalov D and Korobov V I 2014 *Phys. Rev. Lett.* **113** 023004
[12] Karr J Ph 2014 *J. Mol. Spectrosc.* **300** 37
[13] Kajita M, Gopakumar G, Abe M, Hada M and Keller M 2014 *Phys. Rev. A* **89** 032509
[14] Kajita M 2015 *Phys. Rev. A* **92** 043423
[15] Ludlow A D, Boyd M M, Ye J, Peik E and Schmidt P O 2015 *Rev. Mod. Phys.* **87** 637
[16] Olivares Pilón H and Baye D 2013 *Phys. Rev. A* **88** 032502
[17] Olivares Pilón H and Baye D 2012 *J. Phys. B* **45** 065101
[18] O'Halloran M A, Pratt S T, Dehmer P M and Dehmer J L 1987 *J. Chem. Phys.* **87** 3288
[19] Bakalov D, Korobov VI and Schiller S 2011 *J. Phys. B* **44** 025003
[20] Bakalov D and Schiller S 2014 *Appl. Phys. B* **114** 213
[21] Itano W M 2000 *J. Res. Natl. Inst. Stand. Technol.* **105** 829
[22] Dubé P, Madej A A, Bernard J E, Marmet L, Boulanger J S and Cundy S 2005 *Phys. Rev. Lett.* **95** 033001
[23] Dubé P, Madej A A, Zhou Z and Bernard J E 2013 *Phys. Rev. A* **87** 023806
[24] Korobov VI, Hilico L and Karr J Ph 2006 *Phys. Rev. A* **74** 040502(R)
[25] Karr J Ph, Hilico L and Korobov V I 2008 *Phys. Rev. A* **77** 062507
[26] Itano W M, Lewis L L and Wineland D J 1982 *Phys. Rev. A* **25** 1233
[27] Schiller S, Bakalov D, Bekbaev A K and Korobov V I 2014 *Phys. Rev. A* **89** 052521
[28] Rosenband T *et al.* 2007 *Phys. Rev. Lett.* **98** 220801
[29] Chou C W, Hume D B, Koelemeij J C J, Wineland D J and Rosenband T 2010 *Phys. Rev. Lett.* **104** 070802
[30] Huntemann N, Lipphardt B, Okhapkin M, Tamm Chr, Peik E, Taichenachev A V and Yudin V I 2012 *Phys. Rev. Lett.* **109** 213002; Zanon-Willette T, Yudin V I and Taichenachev A V 2015 *Phys. Rev. A* **92** 023416
[31] Keller J, Partner H L, Burgermeister T and Mehlstäubler T E 2015 *J. Appl. Phys.* **118** 104501
[32] Korobov V I, Hilico L and Karr J Ph 2014 *Phys. Rev. Lett.* **112** 103003 and *Phys. Rev. A* **89** 032511
[33] Sturm S, Köhler F, Zatorski J, Wagner A, Harman Z, Werth G, Quint W, Keitel C H and Blaum K 2014 *Nature* **467** 506